Zoological Studies **61**:73 (2022)
doi:10.6620/ZS.2022.61-73

Zoological Studies

Open Access

Finding the Missing Puzzle Piece of the Nisto Stage in the Larval Cycle of the Slipper Lobster *Scyllarides squammosus*: A Molecular and Morphological Approach

Chiho Hidaka[1], Chien-Hui Yang[2], and Kaori Wakabayashi[3,*]

[1]*School of Applied Biological Science, Hiroshima University, Kagamiyama 1-4-4, Higashi-Hiroshima, Hiroshima 739-8528, Japan. E-mail: chihonman67@gmail.com (Hidaka)*
[2]*Institute of Marine Biology and Centre of Excellence for the Oceans, National Taiwan Ocean University, 2 Pei-Ning Road, Keelung 202301, Taiwan. E-mail: chyang@mail.ntou.edu.tw (Yang)*
[3]*Graduate School of Integrated Sciences for Life, Hiroshima University, Kagamiyama 1-4-4, Higashi-Hiroshima, Hiroshima 739-8528, Japan. *Correspondence: E-mail: kaoriw@hiroshima-u.ac.jp (Wakabayashi)*

Received 18 June 2021 / Accepted 2 September 2022 / Published 14 December 2022
Communicated by Benny K.K. Chan

Slipper and spiny lobsters are crustaceans that are in high demand and possess great commercial potential as valuable foods. The early life stages are important to understand the distribution and resource ecology of those lobsters. However, much less information is available about slipper lobsters than spiny lobsters. Biological information concerning the transition stage from the planktonic to the benthic phase, the so-called nisto stage, is limited probably due to its short duration. An individual scyllarid nisto was discovered while scuba diving off Chichijima Island. DNA analyses using mitochondrial 16S rRNA and cytochrome *c* oxidase subunit 1 (*COI*) genes confirmed this specimen to be *Scyllarides squammosus* (H. Milne Edwards, 1837). Detailed morphological observations of this specimen and its comparison with previous reports on *Scyllarides* nistos suggest that the diagnostic character of *S. squammosus* nisto is the pleura of the second to fifth pleonites possessing prominent teeth entirely on the lateral margin. Other morphological characteristics are the carapace with the widest distance in the middle and the second to fifth pleonites bearing two tubercles on each side. This report describes the identification of the first worldwide record of a *Scyllarides* nisto, confirmed by molecular barcoding.

Key words: Decapoda, Taxonomy, Larva, Settlement, DNA barcoding.

BACKGROUND

Scyllaridae, a family of the infraorder Achelata (Decapoda: Crustacea), consists of 91 species and two subspecies assigned to 19 genera in four subfamilies (Holthuis 1991; WoRMS 2021). The family includes approximately 20 lobster species of commercial interest in the following four genera: (1) *Scyllarides*, (2) *Parribacus*, (3) *Ibacus*, and (4) *Thenus* (Holthuis 1991; Spanier and Lavalli 2013). Despite its commercial importance, much fewer studies are available for Scyllaridae, especially in contrast to another family of Achelata, Palinuridae, which includes many highly valuable lobster species (Spanier and Lavalli 2007; Ohta and Uehara 2017). Larval phases are particularly important for understanding the distribution and reproductive efficiency of those lobster species. The scyllarid zoea, called phyllosoma, grows through a series of molting stages and then metamorphoses into the decapodid phase, called the nisto (Martin 2014; Lavalli et al. 2019). A nisto provides the link between the pelagic and benthic phases and then becomes a

Citation: Hidaka C, Yang CH, Wakabayashi K. 2022. Finding the missing puzzle piece of the nisto stage in the larval cycle of the slipper lobster *Scyllarides squammosus*: a molecular and morphological approach. Zool Stud **61**:73. doi:10.6620/ZS.2022.61-73.

juvenile with a single molting (Booth et al. 2005; Sekiguchi et al. 2007). Puerulus, the decapodid phase of palinulids, is known to swim towards the shore from or beyond the continental shelf break (Booth and Phillips 1994), whereas the precise role of the nisto likely varies among the species (Booth et al. 2005; Sekiguchi et al. 2007).

Nisto can be easily distinguished from other decapod planktonic phases by the presence of extremely flattened carapace and antennae. The nisto of each four subfamilies shows specific carapace characteristics, which can also be seen in the adult (Webber and Booth 2007). These characteristics include orbits at extreme anterolateral angles, V-shaped in Theninae (Barnett et al. 1984; Wakabayashi and Phillips 2016), incision at the middle of posterior margin in Scyllarinae (Wakabayashi et al. 2017b 2020), and cervical incision deep in Ibacinae (Takahashi and Saisho 1978; Marinovic et al. 1994; Yoneyama and Takeda 1998), whereas none of those characteristics are found in Arctidinae. The nisto of Arctidinae has another diagnostic character, namely, a strong median carina with a sharp tip on pleonite terga 4 and 5 (Chace Jr 1966; Lyons 1970).

Both biological and ecological studies on the scyllarid nisto should begin with the identification of wild-caught specimens at the species level, but the identification is still in the preliminary stages due to a serious lack of information (Johnson 1975; Wakabayashi et al. 2017b 2020). This issue arises from the short duration of the nisto phase (about a week under culture) and the nisto's unknown settling ground preference, which limits researchers' collection abilities (Sekiguchi et al. 2007). In Arctidinae, complete larval development from hatching to metamorphosis has not been achieved yet in captive rearing, but the duration of the entire planktonic phase is estimated to be 8–9 months, with stages occurring prior to metamorphosis into the nisto stage (Robertson 1969a b; Crosnier 1972; Sekiguchi et al. 2007). Twenty-four nisto specimens from the wild were recorded and assigned to seven species of *Scyllarides* based on how their collection localities accorded with the adult distributions (Guérin-Méneville 1855; Pfeffer 1881; Miers 1882; Bouvier 1913; Barnard 1950; Chace Jr 1966; Michel 1968; Robertson 1968; Lyons 1970; Crosnier 1972; Johnson 1975). However, considering the overlapping distributions among some species of *Scyllarides* (Holthuis, 1991) and the potential of wide dispersal of phyllosoma larvae with a long planktonic life in this genus, the species assignment for the 24 nistos are not fully reliable. Such uncertainty can be solved nowadays by DNA barcoding, which has contribute to correct species identifications in many animals, including marine crustacean larvae (see Chen et al. 2013; Palero et al. 2016; Wakabayashi et al. 2017b 2020; Li et al. 2019; Wong et al. 2021; Ueda et al. 2021; Chow et al. 2022). We recently collected an Arctidinae nisto specimen from an area off the Japanese Ogasawara Islands. Based on molecular evidence, the nisto was confirmed to belong to *Scyllarides squammosus* (H. Milne Edwards, 1837). It is worthwhile to present detailed morphological descriptions of the nisto with a correct identification.

MATERIALS AND METHODS

Sampling

An individual scyllarid nisto was found off Chichijima Island, part of the Ogasawara Islands, Japan (27°04'29.7"N, 142°11'06.3"E) in May 2017 during a scuba diving trip. It was trapped underwater in a plastic bottle after being photographed (Fig. 1) and then fixed with 99% ethanol on land. The depth at which it was found was 8 m, and the water temperature and salinity at the site were 20°C and 35, respectively.

DNA analyses

The sequences of the mitochondrial *COI* gene (*COI*) and 16S rRNA gene (*16S*) regions were used for molecular identification (Hebert et al. 2003; Hajibabaei et al. 2007; Vogler and Monaghan 2007; Bucklin et al. 2011). Genomic DNA was extracted from the fifth pereopod of the nisto specimen (NSMT-Cr 30950) using NucleoSpin Tissue XS (Macherey-Nagel, Germany) according to the manufacturer's protocol. Abdominal muscles of *S. squammosus* (NTOU M00972 and NTOU M02303) were also used for genomic DNA extraction using the QIAGEN® DNeasy Blood and Tissue Kit (Cat. No. 69504, Valencia, CA). The target regions were amplified via a polymerase chain reaction (PCR) with the universal primer pairs, LCO1490/HCO2198 (Folmer et al. 1994) for *COI* and 16Sar-L/16Sbr-H (Palumbi et al. 2002) for *16S* PCR. Cycle sequencings were conducted following the methods described by Yoshimoto et al. (2020) and Yang et al. (2012). The nucleotide sequences of the studied species were deposited through the International Nucleotide Sequence Database Collaboration at the National Center for Biotechnology Information, Bethesda, MD, USA.

Multiple sequence alignment was conducted using MUSCLE with default parameters on MEGA 7 (Kumar et al. 2016). Poorly aligned and non-informative sites on *16S* were removed using Gblocks 0.91b (Castresana 2000). The final lengths of aligned *COI* and *16S* were 500 bp and 413 bp, respectively. MEGA 7 was also used to compute the genetic distances as estimated

with the K2P model (Kimura 1980) among 10 species of Scyllaridae, including all nine species of Arctidinae with available sequences and *Parribacus antarcticus* (Ibacinae) as the outgroup for the phylogenetic tree analysis (Tables 1 and Table S1).

The two sequences of *COI* and *16S* were combined, and a phylogenetic tree was reconstructed using Bayesian inference (BI) based on the combined sequence dataset (*COI+16S*) with a total of 33 sequences (Table 1). Missing data were treated as 'N'. The BI analysis was conducted using MrBayes 3.2.6 (Ronquist et al. 2012). Models of nucleotide evolution for the sequence of *16S* and each codon position of *COI* were determined based on the smallest Akaike Information Criterion (AIC) score on MEGA 7 under default parameters using a neighbor-joining tree. For *COI*, a general time-reversible model with gamma distribution (GTR+G), Hasegawa-Kishino-Yano model (HKY), and GTR+G were determined to be the best-fit models for the first, second, and third codon positions, respectively. For *16S*, GTR with gamma distribution having invariant sites (GTR+G+I) was the best-fit model. A tree search was run for 500,000 generations with trees every 1,000 generations, and the first 125,000 trees were discarded as "burn-in." Support was given as posterior probabilities (Pp) calculated under default parameters. The reconstructed trees were visualized in Figtree v. 1.4.4 (Rambaut 2018).

Morphological description

Appendages were separated from the body under a stereo microscope (SZX-7, Olympus, Japan). The appendages were soaked in lactophenol for 5 to 10 min and then preserved on glass slides in CMCP-10 (Polysciences, Inc., USA), which is a highly viscous mounting medium. Measurements and body drawings were made under the same stereo microscope while using a drawing tube. Observations and drawings of each appendage were made using a compound microscope (BX-51, Olympus, Japan) equipped with a drawing tube. The body length, cephalic length, carapace width, and telson length (BL, CL, CW, and TL, respectively) were defined from the anterior end of the antenna to the posterior end of the telson, from the anterior end to the posterior end of the carapace, the widest distance of the carapace, and from the anterior end to the posterior end of the telson, respectively. Terminology for the scyllarid nisto was based on studies by Wakabayashi et al. (2017b 2020). The drawings were edited using a drawing application ibis Paint X (Ibis inc., Japan).

RESULTS

DNA analyses

The K2P genetic distances of the *COI* within species of the genus *Scyllarides* were 2.5% or lower (0%–0.6% in *S. squammosus*, 0.4% in *S. brasiliensis*, and 0%–2.5% in *S. latus*) except in *S. haanii* (0.6%–11.3%). Distances between species of this genus ranged from 4.4% to 21.1% (Table S1). For *16S*, the K2P distances within the *Scyllarides* species were 0%–0.7% in *S. squammosus* and 0%–1.0% in both *S. latus* and *S.*

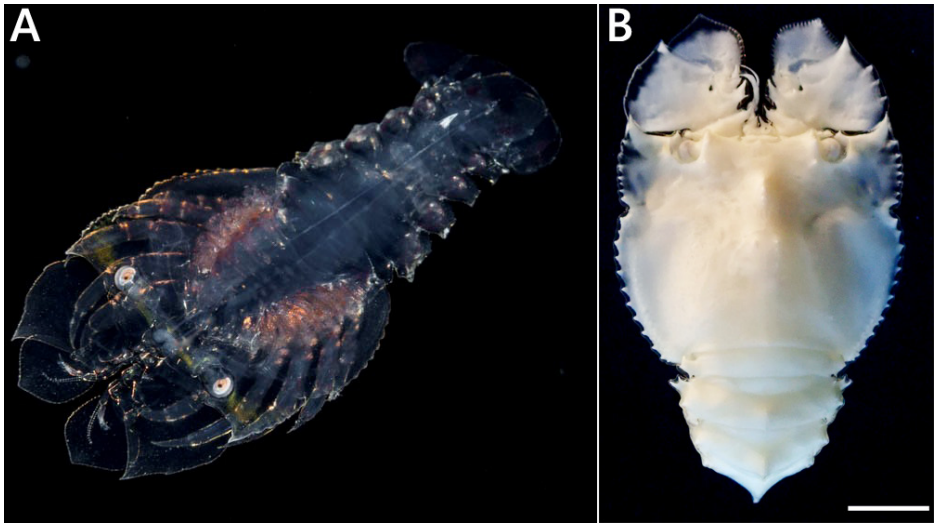

Fig. 1. *Scyllarides squammosus* (H. Milne Edwards, 1837), nisto. A: *in situ*, live (photographed by Hideki Abe, reproduced with permission from Wakabayashi et al. 2017a, p. 59 in which the nisto was named as *Scyllarides* sp.); B: fixed specimen (NSMT-Cr 30950) in 99% ethanol. Scale bar = 5 mm.

haanii. Our nisto specimen showed the K2P distances of 0.2%–0.6% for *COI* and 0.2%–1.0% for *16S* from *S. squammosus*, respectively (Table S1). Two Hawaiian and Chilean specimens of *Arctides regalis* showed a K2P distance of 0%–0.6% for both gene regions, but the specimen from Réunion had a distance of 5.3% to 5.5% for *COI* and 3.3% for *16S* from the former specimens. The K2P distances between our nisto and the species of *Arctides* were greater than 20% and 12% for *COI* and *16S*, respectively.

The BI tree demonstrated that the conspecific sequences were monophyletic (Fig. 2). The nisto specimen examined in this study was placed in a clade with *S. squammosus* with strong support (Pp = 1).

TAXONOMY

Order DECAPODA Latreille, 1802
Family SCYLLARIDAE Latreille, 1825

Table 1. List of arctinid species and outgroup lobster used for DNA analyses

Species	Voucher	Locality	GenBank Accession Nos.		Source
			COI	*16S*	
Scyllaridae					
Arctidinae					
Scyllarides squammosus	NTOU M02303	Hepingdao, Taiwan	OP379522	OP379972	this study
	NTOU M00972	Market in Taiwan	JN701654	JN701689.2	Yang et al. (2012)
	n.a.	China	MK783265 *	MK783265 *	Liu et al. (2019)
	n.a.	South Africa	KX275388 [#1]	-	Singh et al. (2017)
(nisto)	NSMT-Cr 30950	Ogasawara, Japan	OP379523	OP379973	this study
(phyllosoma)	NHMUK-2015.3285	Coral Sea	KX373667 [#2]	-	Palero et al. (2016)
(phyllosoma)	n.a.	East Australian Sea	MK371349 [#3]	-	Woodings et al. (2019)
(phyllosoma)	n.a.	East Australian Sea	MK371352 [#4]	-	Woodings et al. (2019)
Scyllarides brasiliensis	KC6292	n.a.	KF827966	KF828186	Bracken-Grissom et al. (2014)
	n.a.	Brazil	JX896701 [#5]	-	Rodríguez-Rey et al. (2014)
	n.a.	Brazil	JX896724 [#6]	-	Rodríguez-Rey et al. (2014)
Scyllarides haanii	n.a.	n.a.	MN817127 *	MN817127 *	Liu et al. (unpubl.)
	KC6018	Hawaii, USA	JN701656	JN701690	Yang et al. (2012)
	KC6019	Hawaii, USA	-	JN701691[Δ1]	Yang et al. (2012)
	NTOU M00973	Taiwan	JN701655 [#7]	-	Yang et al. (2012)
	n.a.	Easter Island, Chile	MW699539 [#8]	-	Báez et al. (2022)
Scyllarides deceptor	CCDB BRA 4190	Brazil	MF490045	MF490148	Mantelatto et al. (2017)
Scyllarides latus	n.a.	n.a.	KC107814 *	KC107814 *	Shen et al. (2013)
	FP0014	n.a.	FJ174947	FJ174907	Palero et al. (2009)
	JSDAz37	Portugal	JQ306108 [#9]	-	Matzen da Silva et al. (2011)
	n.a.	n.a.	JQ623990 [#10]	-	Keskin (unpubl.)
	n.a.	Izmir Bay, Turkey	KC311420 [#11]	-	Keskin and Atar (2013)
	n.a.	Portugal	JF928188 [#12]	-	Froufe et al. (2019)
	n.a.	n.a.	-	DQ377974[Δ2]	Cannas et al. (unpubl.)
Scyllarides herklotsii	ICMD 2301998	Eastern Atlantic Ocean	FJ174946	FJ174906	Palero et al. (2009)
Scyllarides nodifer	ULLZ7845	Northern Gulf of Mexico, USA	JN701657	JN701692	Yang et al. (2012)
	n.a.	Gulf of Mexico, USA	-	U96088[Δ3]	Tam and Kornfield (1998)
Arctides antipodarum	KC6076	Australia	-	JN701688[Δ4]	Yang et al. (2012)
Arctides regalis	MNHN-IU-2009-462	Réunion	JN701651	JN701685	Yang et al. (2012)
	KC6004	Hawaii, USA	JN701653	JN701687	Yang et al. (2012)
	KC6003	Hawaii, USA	JN701652	JN701686	Yang et al. (2012)
	n.a.	Chile	MW699538 [#13]	-	Araneda et al. (unpubl.)
Ibacinae					
Parribacus antarcticus	NTOU M00975	Taiwan	JN701666	JN701701	Yang et al. (2012)

n.a.: not available. See figure 2 caption for the meaning of hash (#), delta (Δ), and asterisk (*) symbols.

Genus *Scyllarides* Gill, 1898
Scyllarides squammosus (H. Milne Edwards, 1837)
Nisto

Material examined: Nisto, NSMT-Cr 30950, BL = 39 mm, CL = 14.5 mm, CW = 17 mm, TL = 9 mm.

Description: Carapace (Fig. 3A, 3B): Wider than longer (CW/CL 1.17) with maximum width in the middle; surface with few tubercules, entirely furnished with fine setae; anterior margin smooth, a prominent horn present at both angles; lateral margin possessing a distinct post-cervical incision, with 8 (right) to 9 (left) anterolateral and 14 (right) to 12 (left) post-lateral teeth; rostral short with blunt end; 2 prominent tubercules and 1 small tubercule on the inner and posterior edges of orbits; gastric tooth possessing 2 prominent tubercles anteriorly and 4 small setae posteriorly; cardiac tooth bearing 2 rows of prominent tubercules anteriorly and 2 rows of small setae posteriorly, cardiac ridge with small setae; 10 small setae (8 each on the right and left sides, 2 in the middle) present along the post-cervical groove; 10 small setae in a row along post-lateral teeth; 5 small setae present at middle of posterior margin.

Antennule (Fig. 4A): Peduncle 3-segmented with flagellated distal end; proximal segment bearing dense long setae on ventral side; second segment possessing small setae scattered; third segment almost naked; accessory flagellum 18-articulated as long as the primary flagellum; primary flagellum thicker than accessory flagellum, 15-articulated, group of aesthetascs present on articles 5–12.

Antenna (Fig. 3A): 4-segmented, biramous, broad, flat; proximal segment inverted triangle, anterior margin with a ridge at middle; second segment with serrated lateral margin, prominent horn at anterolateral angle, a small notch on anteromedial margin, 2 small teeth on medial margin; third segment bearing a prominent tooth on anteromedial angle; distal segment surrounded with finely serrated margins.

Mandible (Fig. 4B): Poorly developed, slightly

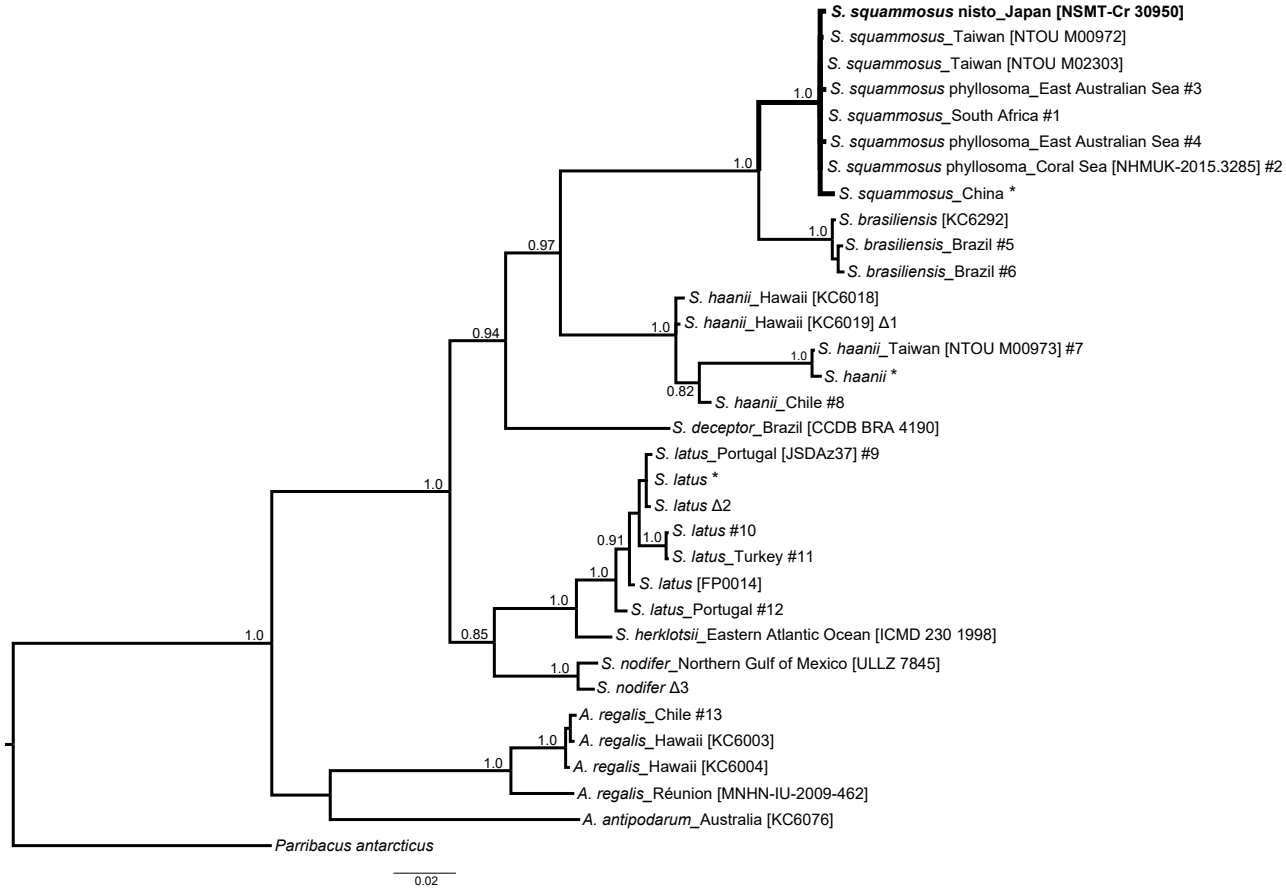

Fig. 2. Bayesian phylogenetic tree of the subfamily Arctidinae with partial sequences of *COI* and *16S*. Posterior probability (Pp) values are shown when above 0.8. The tree was constructed basically with both the *COI* and *16S* sequences, but the operational taxonomic units (OTUs) with hash (#) were inferred only from the *COI* and those with delta (Δ) were inferred only from the *16S*, due to a lack of information. Asterisks (*) indicate the OTUs with sequences resulting from the mitogenome.

asymmetrical; palp present.

Maxillule (Fig. 4C): Uniramous; poorly developed; basal endite with 5 small tubercules on anterior margin; coxal endite unarmed on anterior margin, bearing 3 small setae on basal part.

Maxilla (Fig. 4D): Flattened; endopod slightly differentiated with 8 setae and 3 small spines on the medial margin; endites differentiated, 4 (2+2) and 7 (5+2) setae on anterior ends of coxal and basal endites, 1 and 2 setae present on the inner proximal parts of coxal and basal endites, respectively; hair-like setae lining the outer margin of scaphognathite.

First maxilliped (Fig. 4E): Biramous, coxa and basis undifferentiated, flattened; endopod unsegmented, smooth; exopod with 15 marginal setae on proximal part, small setae on distal end; epipod membranous, expanding posteriorly, bearing 5 long setae; 2 small setae present at the distal end of basal endite.

Second maxilliped (Fig. 4F): Biramous, coxa and basis undifferentiated; endopod 4-segmented with 0,1,13,0 setae; exopod incompletely segmented, longer than endopod, 2 small setae at distal end.

Third maxilliped (Fig. 4G): Biramous, coxa and basis differentiated; endopod 5-segmented, carpus with dense setae (~30), propodus with 14 setae, dactylus with 4 long setae on inner margin; exopod segmented, poorly developed with 7 small setae on distal end.

Pereiopods (Fig. 5A): Pereiopods 1–4 biramous, coxa and basis differentiated, endopods 5-segmented with almost equal length, exopods degenerated, merus and carpus bearing a prominent horn at distal end, ischium of pereiopod 2–4 with 4 small spines; Pereiopod 5 uniramous, shortest, merus possessing a prominent horn at the distal end, ischium bearing a conspicuous spine pointing posteriorly.

Pleon (Fig. 3A, 3B): Tergum of pleonite 1 smooth; median carina distinct on tergites of pleonites 2–5; terga of pleonites 2–3 with a few spicules, small spines on median carina, a small tooth at center of posterior margin; terga of pleonites 4–5 smooth, a large tooth present at center of posterior margin; pleura of pleonites 2–5 serrated with large tooth, 2 small spines on the medial margins of pleura.

Pleopods (Fig. 5B): Present on pleonites 2–5; biramous; 2 setae at medial distal angle of protopod; exopod surrounded with 35 (pleopod 1), 37 (2), 38 (3), 33 (4) long plumose natatory setae, each possessing 6 (pleopod 1), 12 (2), 14 (3), 12 (4) small plumose setae at distal end; endopod surrounded with 48 (pleopod 1), 52 (2), 48 (3), 48 (4) long plumose natatory setae, each possessing 0 (pleopod 1), 2 (2), 5 (3), 4 (4) small plumose setae at distal end, appendix interna not reaching distal end of endopod, with approximately 12 cincinnuli at the tip, a plumose seta present just beside the cincinnuli for pleopods 2 and 4.

Uropod (Fig. 5C): A tooth present at lateral

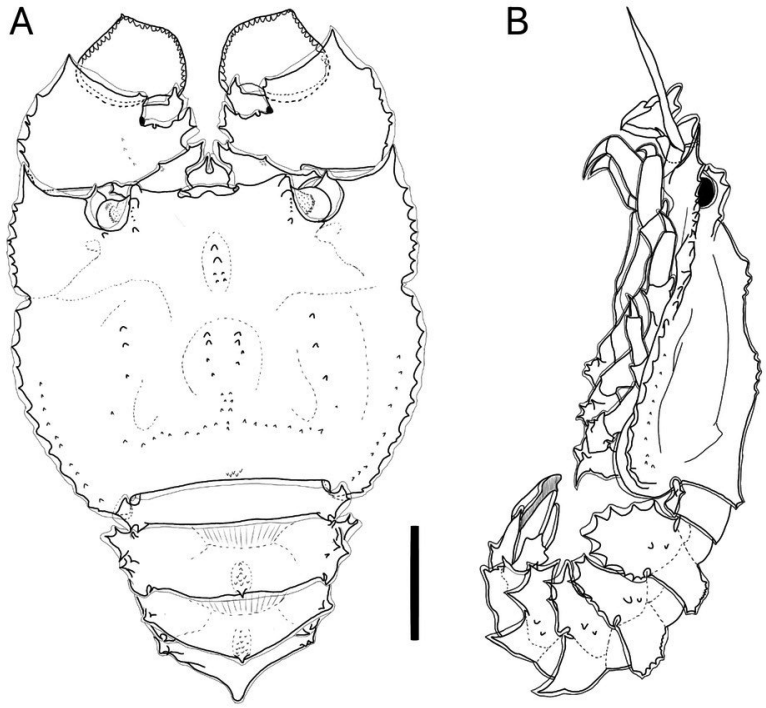

Fig. 3. *Scyllarides squammosus* (H. Milne Edwards, 1837), nisto. A: Body, dorsal, a pair of antennules omitted; B: Body, lateral (left), ventral side of telson in gray. Scale bar = 5 mm.

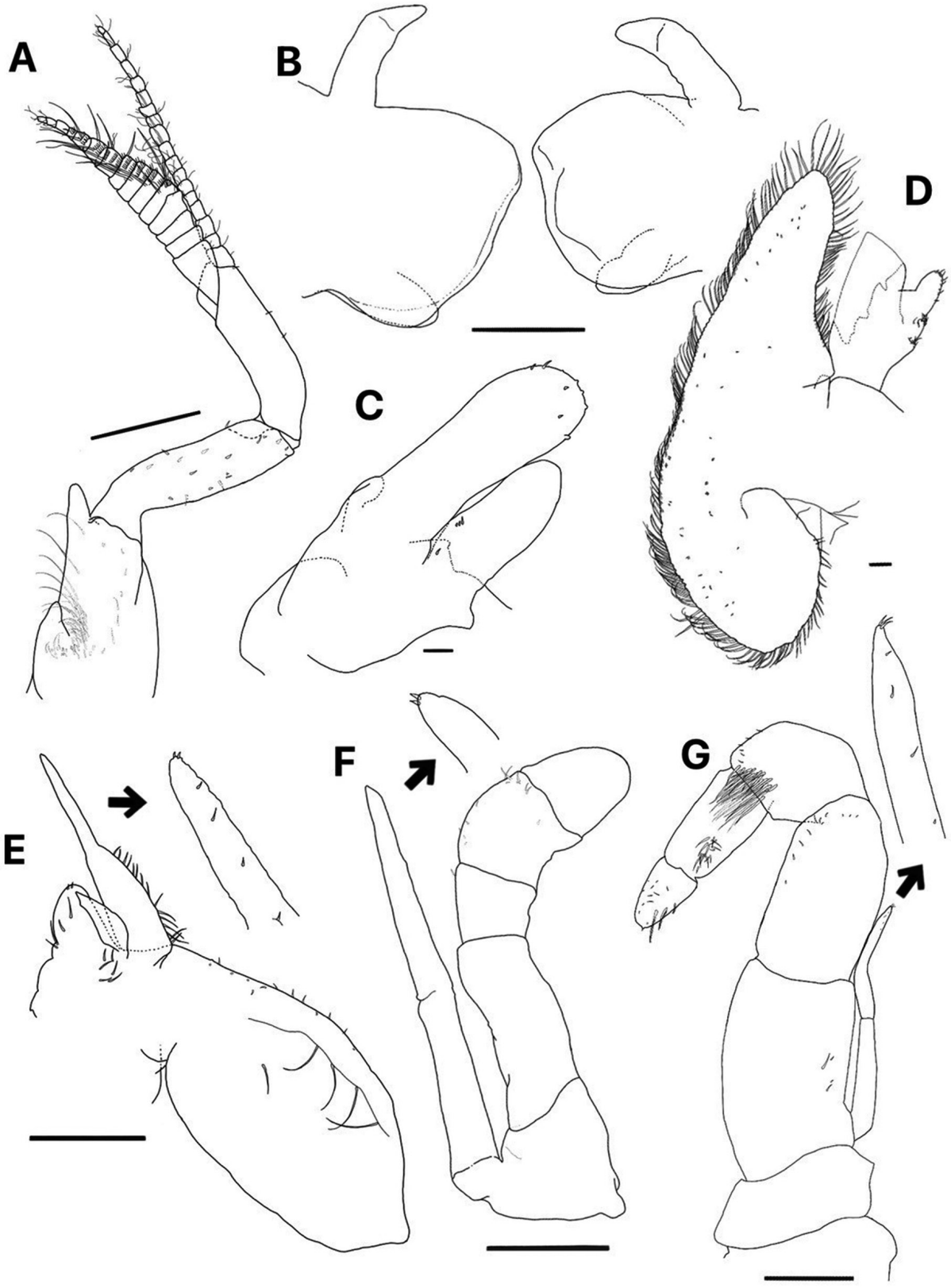

Fig. 4. *Scyllarides squammosus* (H. Milne Edwards, 1837), nisto. A: Antennule, right, ventrolateral; B: Mandibles, ventral; C: Maxillule, right, ventral; D: Maxilla, right, ventral; E: First maxilliped, right, dorsal; F: Second maxilliped, right, ventral; G: Third maxilliped, right, dorsal. Scale bars: A, E, G = 1 mm; B, F = 0.5 mm; C, D = 0.1 mm.

margins of exopod and endopod; medial margin of endopod serrated.

Telson (Fig. 5D): A tooth present at the proximal, lateral margins.

Color (Fig. 1): Body entirely transparent in live specimen except a yellow line along the anterior margin of carapace and gills in pink. Specimen preserved in ethanol entirely white with transparent body margins.

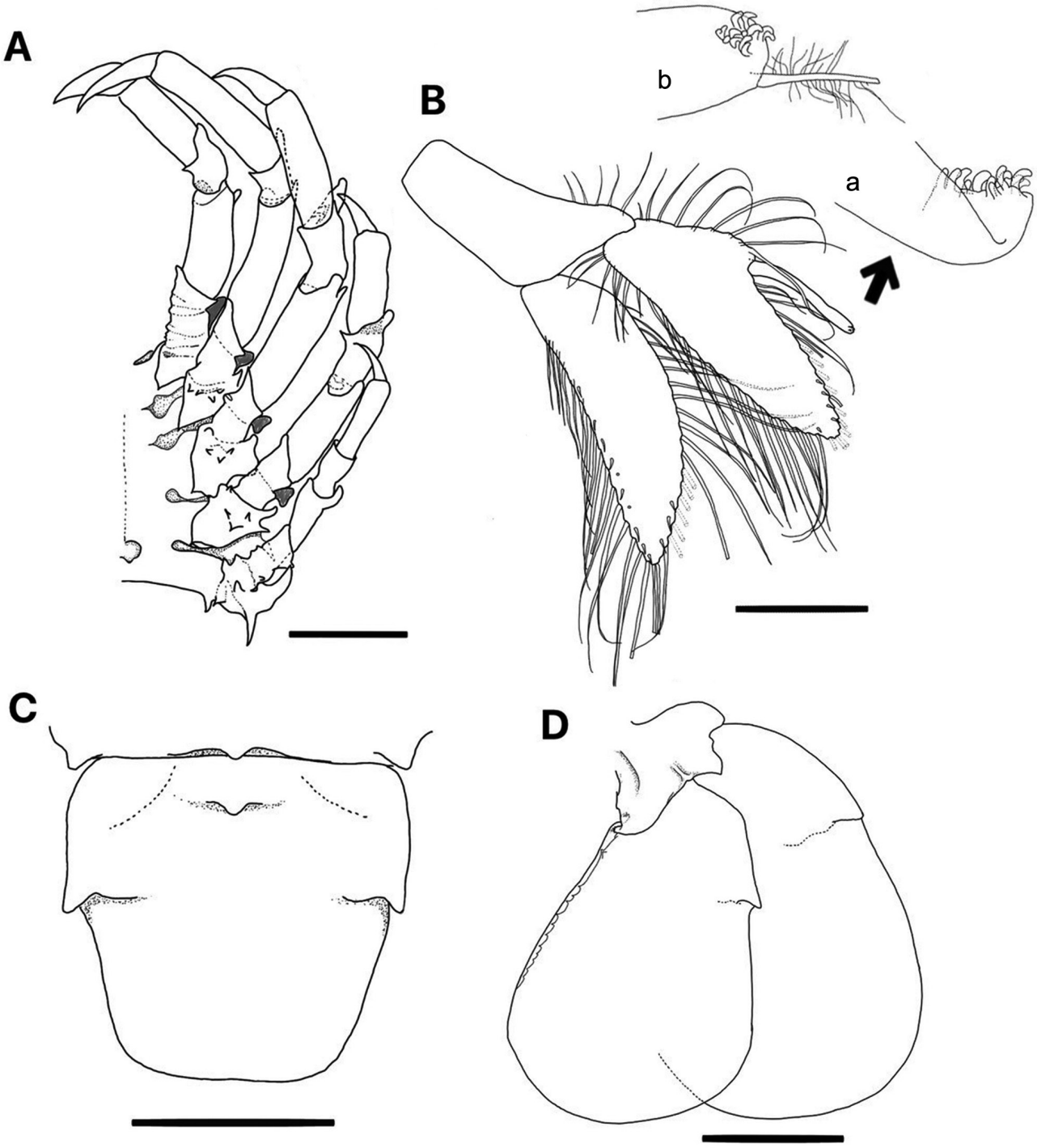

Fig. 5. *Scyllarides squammosus* (H. Milne Edwards, 1837), nisto. A: Pereiopods, left, ventral, degenerated exopods shown in shaded; B: Pleopod 3, right, anterior, with enlarged distal ends of pleopods 1 and 3 (a) and pleopods 2 and 4 (b); C: Telson, dorsal; D: Uropod, right, dorsal. Scale bars: A, D = 3 mm; C = 2 mm, B = 1 mm.

DISCUSSION

The nisto specimen showing the morphological features of the subfamily Arctidinae collected off the coast of the Ogasawara Islands was confirmed to be *S. squammosus* based on DNA analyses. Although the larval development of the planktonic phase has been well documented in this species, the transition phase has scarcely been recognized. Mid to late development from stages VI to XII (final) was illustrated based on wild-caught specimens (Michel 1968; Johnson 1971 1977; Palero et al. 2016; Chow et al. 2022), and the identities of larval specimens examined by Palero et al. (2016) and Chow et al. (2022) were confirmed based on molecular evidence. This study finally found the missing puzzle piece in the early life history of *S. squammosus* with the description of the nisto stage, which plays a role in the species' transition from planktonic to benthic life. Captive breeding of this species was attempted by Saisho and Sone (1971) using *Artemia* as food, and they described the early larval development from newly hatched phyllosoma to instar 6. The youngest larva of *S. squammosus* collected from the wild assessed as stage VI (Palero et al. 2016) was much more developed than the larva at instar 6 (Saisho and Sone 1971), suggesting that several stages in the early development of this species are still missing.

The adult *S. squammosus* inhabits oceanic reefs and is widely distributed in the Indo-West Pacific from the Hawaiian Islands to the east coast of Africa (Holthuis 1991). In Japan, this species has been found south of the Boso Peninsula, Chiba Prefecture, and the Ryukyu and Ogasawara Archipelagoes (Miyake 1982; Nishikiori and Sekiguchi 2001). Indeed, the presence of the berried females of this species have been confirmed off the coast of Chichijima Island (Nishikiori and Sekiguchi 2001) from which our nisto specimen was found. This particular nisto probably reached the coastal area of Chichijima Island to seek ground for settlement. Since another species, *S. haanii*, is also present off Chichijima Island (Nishikiori and Sekiguchi 2001), the nisto found off the Ogasawara Islands could either be *S. squammosus* or *S. haanii*. Genetic distances between the two species are greater than 15.7% for *COI* and 10.8% for *16S*; thus, the two species could be clearly distinguished using the K2P genetic distance. The species with the closest genetic distance from our nisto specimen (*S. squammosus*) is *S. brasiliensis*. The adult *S. brasiliensis* is distributed in the Southern Atlantic from Brazil (the States of Maranhão to Bahia) to the Dominican Republic (Holthuis 1991). It is hard to believe that a nisto of *S. brasiliensis* could be found off the Ogasawara Islands.

Nisto has been described for seven out of 14 species of the genus *Scyllarides*, although all previous descriptions had been based on wild-caught specimens that had not undergone molecular identification. Our nisto specimen agreed well with the description of a nisto identified as *S. squammosus* recorded from off the coast of New Caledonia (Michel 1968), as both nistos possess pleurae 2 to 5 surrounded by large sharp teeth on both the anterior and posterior margins, though minor differences between them are also present in body length and CW/CL ratio. Michel's nisto is probably *S. squammosus*, after considering the morphological similarity to our nisto. Nevertheless, we cannot eliminate the possibility of other species with similar morphology and minor size differences, since the existence of undescribed species in the Pacific Ocean that are closely related to *S. squammosus* has been suggested (Chow et al. 2022). *Pseudibacus pfefferi* (Miers, 1882) collected from off Mauritius is considered the nisto stage of *S. squammosus* (Bouvier 1913). However, it is hard to assess whether *P. pfefferi* is likely this species due to an ambiguous description for the pleurae. Pleura 2 of the nisto of *S. nodifer* is distally subacute with a small spine at the posterior angle and a blunt spine at the anterior angle (Lyons 1970). The posterior margin of pleura 2 is smooth in the nistos of *S. herklosti* (Chace Jr 1960; Crosnier 1972) and *S. astori* (Johnson 1975). In the nisto of *S. aequinoctialis*, six rounded teeth are present on the anterior margin of pleura 2 with an acute spine at the lower extremity, and the upper third of posterior margin bears seven rounded or smooth teeth (Lyons 1970). *Pseudibacus gerstaeckeri* (Pfeffer 1881) was assigned to the nisto stage of *S. aequinoctialis* (Bouvier 1913) after which its certainty was morphologically confirmed (Lyons 1970). Guérin-Méneville (1855) described that all pleurae of *Pseudibacus veranyi* [identified as *S. latus* by Bouvier (1913)] are scalloped and prickly with teeth of different sizes and arrangements. The CW/CL is 1.5 in *S. aequinoctialis* (calculated based on Lyons's illustration), whereas that value is 1.2 to 1.3 in other species, including our nisto specimen. The nisto of *S. nodifer* has a low blunt tubercle on the medial margins of pleura, while our nisto presented two lows of blunt tubercles. The nisto described by Barnard (1950) that was later identified as *S. elisabethae* by Chace Jr (1966) has a carapace with its widest distance on the anterior margin. The nistos of other species show the widest distance on the middle part of carapace.

Several diagnostic characteristics are known to distinguish the adult specimens of *Scyllarides* from those of *Arctides*: (1) ornamental patterns on carapace and pleonites (tubercules in *Scyllarides* versus spines in *Arctides*), (2) transverse groove on tergum of pleonite 1 (absent in *Scyllarides* versus present in *Arctides*),

and (3) postorbital spine (absent in *Scyllarides* versus present in *Arctides*) as described by Holthuis (1991) and Webber and Booth (2007). Tubercules and spines were not developed in the nisto found in this study; thus, the ornamental patterns on carapace and pleonites may not be useful for distinguishing between the two genera. Our nisto specimen did not show postorbital spines and a transverse groove on its tergum of pleonite 1, a finding consistent with the adult characteristics of *Scyllarides*. However, the morphological features are not always fully developed in the nisto (Wakabayashi et al. 2017b 2020), and it is still unknown whether the absence/presence of postorbital spines and transverse groove on pleonite 1 is useful for identifying the genus of nisto specimens. Examinations of the *Arctides* nisto (which has not yet been described) would clarify the usefulness of these characters.

Our DNA analyses also provide a note on the taxonomic status of *S. haanii*. The K2P analysis of *COI* sequences suggest that a genetic distance of 2.5% could be used as an indicator of the maximum intraspecific threshold within the species of *Scyllarides*. The closest interspecific distances are 4.2%–4.8% between *S. herklotsii* and *S. latus*, and the greatest distances are 18.1%–21.1% between *S. brasiliensis* and *S. latus*. The distances within *S. haanii* ranged from 0.6% to 11.3%, indicating the possibility of the existence of a cryptic species in *S. haanii*. The BI phylogenetic tree also strongly suggests the presence of several clades within *S. haanii*. Future population genetic analysis may reveal the correct identities of both the Hawaiian and East Asian populations of *S. haanii*.

Acknowledgments: The authors express their gratitude to Mr. Osamu Morishita (Diving shop Urashiman) and Mr. Hideki Abe (Hideki Abe Photo Office) for their kindness of providing the specimen and underwater photograph. This work was partly supported by Grant-in-aid for the Promotion of Joint International Research (Fostering Joint International Research) (KAKENHI no. 17KK0157).

Authors' contributions: Chiho Hidaka and Kaori Wakabayashi designed the study. Chiho Hidaka made the morphological observations. Chiho Hidaka and Chien-Hui Yang conducted the molecular analyses. Chiho Hidaka and Kaori Wakabayashi wrote the first draft of the manuscript, and all the authors read, improved, and approved the manuscript.

Competing interests: All the authors declare that they have no conflict of interest.

Availability of data and materials: The nucleotide sequence data are available in the GenBank, National Center for Biotechnology Information. Other data that support the findings of this study are available from the corresponding author upon request.

Consent for publication: Not applicable.

Ethics approval consent to participate: Not applicable.

REFERENCES

Báez P, Araneda C, Burns L, Navarrete C. 2022. First record and distributional extension to Rapa Nui (Easter Island) of the slipper lobster *Scyllarides haanii* (Crustacea, Decapoda, Scyllaridae). Lat Am J Aquat Res **50(1):**139–143. doi:10.3856/vol50-issue1-fulltext-2765.

Barnard KH. 1950. Descriptive Catalogue of South African Decapod Crustacea. Annal South African Mus **38:**1–837.

Barnett BM, Hartwick RF, Milward NE. 1984. Phyllosoma and nisto stage of the Morton Bay bug, *Thenus orientalis* (Lund) (Crustacea: Decapoda: Scyllaridae), from shelf waters of the Great Barrier Reef. Mar Freshw Res **35(2):**143–152. doi:10.1071/MF9840143.

Booth JD, Phillips BF. 1994. Early life history of spiny lobster. Crustaceana **66(3):**271–294. doi:10.1163/156854094X00035.

Booth JD, Webber WR, Sekiguchi H, Coutures E. 2005. Diverse larval recruitment strategies within the Scyllaridae. NZ J Mar Freshw Res **39(3):**581–592. doi:10.1080/00288330.2005.9517337.

Bouvier MEL. 1913. Sur les genres Pseud ibacus et Nisto, et le stade natant des Crustacés décapodes macroures de la famille des Scyllarùlés. CR Hebd Acad Sci **156(22):**1643–1648.

Bracken-Grissom HD, Ahyong ST, Wilkinson RD, Feldmann RM, Schweitzer CE, Breinholt JW, Bendall M, Palero F, Chan TY, Felder DL, Robles R, Chu KH, Tsang LM, Kim D, Martin JW, Crandall KA. 2014. The emergence of lobsters: phylogenetic relationships, morphological evolution and divergence time comparisons of an ancient group (Decapoda: Achelata, Astacidea, Glypheidea, Polychelida). Syst Biol **63(4):**457–479. doi:10.1093/sysbio/syu008.

Bucklin A, Steinke D, Blanco-Bercial L. 2011. DNA barcoding of marine metazoa. Ann Rev Mar Sci **2011(3):**471–508. doi:10.1146/annurev-marine-120308-080950.

Castresana J. 2000. Selection of conserved blocks from multiple alignments for their use in phylogenetic analysis. Mol Biol Evol **17(4):**540–552. doi:10.1093/oxfordjournals.molbev.a026334.

Chace Jr FA. 1966. Decapod crustaceans from St. Helena Island, South Atlantic. Proc US Nat Mus **118(3536):**623–661. doi:10.5479/si.00963801.118-3536.623.

Chen HN, Hoeg JT, Chan BKK. 2013. Morphometric and molecular identification of individual barnacle cyprids from wild plankton: an approach to detecting fouling and invasive barnacle species. Biofouling **29(2):**133–145. doi:10.1080/08927014.2012.753061.

Chow S, Konishi K, Yanagimoto T. 2022. Identification of phyllosoma larvae of the slipper lobster (Family Scyllaridae). 3. Genus *Scyllarides*. Aquat Anim **2022:**AA2022-3. doi:10.34394/aquaticanimals.2022.0_AA2022-3. (in Japanese with English abstract)

Crosneir A. 1972. Naupliosoma, phyllosomes et pseudibacus de *Scyllarides herklosti* (Herklots) (Crustacea, Decapoda, Scyllaridae) récoltés par l'ombango dans le sud du golfe de

guinée. Cah ORSTOM Sér Océanogr **10(2):**139–149.
Folmer O, Black M, Hoeh W, Lutz R, Vrijenhoek R. 1994. DNA primers for amplification of mitochondrial cytochrome *c* oxidase subunit I from diverse metazoan invertebrates. Mol Mar Biol Biotech **3(5):**294–299.
Froufe E, Cabezas P, Alexandrino P, Pérez-Losada M. 2019. Comparative phylogeography of three Achelata lobster species from Macaronesia (North East Atlantic). *In*: Phylogeography and Population Genetics in Crustacea, Chapter 7, pp. 1–19. doi:10.1201/b11113.
Guérin-Ménéville M. 1855. Notice sur un nouveau genre de Crustacés de la tribudes Scyllariens, découvert par M. Verany, aux environs de Nice. Rev Mag Zool Appl Ser 2 **7:**137–141, pl 5.
Hajibabaei M, Singer GAC, Hebert PDN, Hickey DA. 2007. DNA barcoding: how it complements taxonomy, molecular phylogenetics and population genetics. Trend Genet **23(4):**167–172. doi:10.1016/j.tig.2007.02.001.
Hebert PDN, Ratnasingham S, de Waard JR. 2003. Barcoding animal life: cytochrome *c* oxidase subunit 1 divergences among closely related species. Proc Roy Soc London B **270:**S96–99. doi:10.1098/rsbl.2003.0025.
Holthuis LB. 1991. Marine Lobsters of the World. FAO Species Catalogue **13:**1–292.
Johnson MW. 1971. The phyllosoma larvae of slipper lobsters from the Hawaiian Islands and adjacent areas (Decapoda, Scyllaridae). Crustaceana **20(1):**77–103. doi:10.1163/156854071X00544.
Johnson MW. 1975. The postlarvae of *Scyllarides astori* and *Evibacus princeps* of the eastern tropical pacific (Decapoda, Scyllaridae). Crustaceana **28(2):**139–144. doi:10.1163/156854075X00685.
Johnson MW. 1977. The final phyllosoma larval stage of the slipper lobster *Scyllarides squamosus* (H. Milne Edwards) from the Hawaiian Islands (Decapoda, Scyllaridae). Bull Mar Sci **27(2):**338–340.
Keskin E, Atar HH. 2013. DNA barcoding commercially important aquatic invertebrates of Turkey. Mitochondr DNA **24(4):**440–450. doi:10.3109/19401736.2012.762576.
Kimura M. 1980. A simple method for estimating evolutionary rates of base substitutions through comparative studies of nucleotide sequences. J Mol Evol **16(2):**111–120. doi:10.1007/BF01731581.
Kumar S, Stecher G, Tamura K. 2016. MEGA 7: Molecular Evolutionary Genetics Analysis version 7.0 for bigger datasets. Mol Biol Evol **33(7):**1870–1874. doi:10.1093/molbev/msw054.
Lavalli KL, Spanier E, Goldstein JS. 2019. Scyllarid lobster biology and ecology. *In*: Crustacea, pp. 1–26. doi:10.5772/intechopen.88218.
Li JJ, Shih YJ, Ho PH, Jiang GC. 2019. Description of the first zoea of the cavernicolous crab *Karstama boholano* (Ng, 2002) (Crustacea: Decapoda: Sesarmidae) from Taiwan, with notes on ecology. Zool Stud **58:**36. doi:10.6620/ZS.2019.58-36.
Liu H, Yang M, He Y. 2019. Complete mitochondrial genome of blunt slipper lobsters *Scyllarides squammosus* (H. Milne Edwards, 1837). Mitochondr DNA Part B **4(2):**2299–2300. doi:10.1080/23802359.2019.1627935.
Lyons WG. 1970. Scyllarid lobsters (Crustacea, Decapoda). Mem Hourglass Cruises **1(4):**1–74.
Mantelatto FL, Terossia M, Negria M, Buranellia RC, Roblesa R, Magalhãesa T, Tamburusa AF, Rossia N, Miyazakia MJ. 2017. DNA sequence database as a tool to identify decapod crustaceans on the São Paulo coastline. Mitochondr DNA Part A **29(5):**805–815. doi:10.1080/24701394.2017.1365848.
Marinovic B, Lemmens JWT, Knott B. 1994. Larval development of *Ibacus peronii* Leach (Decapoda: Scyllaridae) under laboratory conditions. J Crustac Biol **14(1):**80–96. doi:10.1163/193724094X00498.
Martin JW. 2014. Introduction to the Decapoda. *In*: Atlas of Crustacean Larvae, pp. 230–234.
Matzen da Silva J, Creer S, dos Santos A, Costa AC, Cunha MR, Costa FO, Carvalho GR. 2011. Systematic and evolutionary insights derived from mtDNA COI barcode diversity in the Decapoda (Crustacea: Malacostraca). PLoS ONE **6(5):**e19449. doi:10.1371/journal.pone.0019449.
Michel A. 1968. Les larves phyllosomes et la post-larve de *Scyllarides squamosus* (H. Milne Edwards) — Scyllaridae (Crustacés Décapodes). Cah ORSTOM Sér Océanogr **6(3–4):**139–149.
Miers EJ. 1882. On crustaceans from the Mauritius.—part II. Proc Zool Soc London **50(3):**538–543.
Miyake S. 1982. Japanese Crustacean Decapods and Stomatpods in Color. Vol. 1. Macrura, Anomura and Stomatopoda. Osaka: Hoikusha Publishing. (in Japanese)
Nishikiori K, Sekiguchi H. 2001. Spiny lobster fishery in Ogasawara (Bonin) Islands, Japan. Bull Jap Soc Fish Oceanogr **65(3):**94–102. (in Japanese)
Ohta I, Uehara M. 2017. Fisheries and reproductive biology of spiny and slipper lobsters around Okinawa Islands: Implication for fisheries management. Ann Rep Okinawa Pref Fish Res Ext Cent **76:**31–44. (in Japanese)
Palero F, Genis-Armero R, Hall MR, Clark PF. 2016. DNA barcoding the phyllosoma of *Scyllarides squammosus* (H. Milne Edwards, 1837) (Decapoda: Achelata: Scyllaridae). Zootaxa **4139(4):**481–498. doi:10.11646/zootaxa.4139.4.2.
Palero F, Guerao G, Clark PF, Abelló P. 2009. The true identities of the slipper lobsters *Nisto laevis* and *Nisto asper* (Crustacea: Decapoda: Scyllaridae) verified by DNA analysis. Invertebr Syst **23(1):**77–85. doi:10.1071/IS08033.
Palumbi SR, Martin A, Romano S, McMillan WO, Stice L, Grabowski G. 2002. The Simple Fool's Guide to PCR. Version 2.0. Honolulu: Department of Zoology and Kewalo Marine Laboratory, University of Hawaii.
Pfeffer G. 1881. Die Panzerkrebfe des Hamburger Mufeums. Verh Naturwiss Vereins Hambrug n.f. **5:**22–54.
Rambaut A. 2018. FigTree v1.4.4. Institute of Evolutionary Biology, University of Edinburgh, Edinburgh.
Robertson PB. 1968. The larval development of some western Atlantic lobsters of the family Scyllaridae. The University of Miami, Coral Gables, Florida, USA.
Robertson PB. 1969a. The early larval development of the scyllarid lobster *Scyllarides aequinoctialis* (Lund) in the laboratory, with a revision of the larval characters of the genus. Deep Sea Res **16(6):**557–586. doi:10.1016/0011-7471(69)90059-X.
Robertson PB. 1969b. Biological investigations of the deep sea. No. 48. Phyllosoma larvae of a scyllarid lobster, *Arctides guineensis*, from the western Atlantic. Mar Biol **4:**143–151. doi:10.1007/BF00347040.
Rodríguez-Rey GT, Solé-Cava AM, Lazoski C. 2014. Genetic homogeneity and historical expansions of the slipper lobster, *Scyllarides brasiliensis*, in the south-west Atlantic. Mar Freshw Res **65(1):**59–69. doi:10.1071/MF12359.
Ronquist F, Teslenko M, van der Mark P, Ayres DL, Darling A, Höhna S, Larget B, Liu L, Suchard MA, Huelsenbeck JP. 2012. MrBayes 3.2: Efficient Bayesian phylogenetic inference and model selection across a large model space. Syst Biol **61(3):**539–542. doi:10.1093/sysbio/sys029.
Saisho T, Sone M. 1971. Notes on the early development of a scyllarid lobster, *Scyllarides squamosus* (H. Milne-Edwards). Mem Fac Fish Kagoshima Univ **20(1):**191–196.
Sekiguchi H, Booth JD, Webber WR. 2007. Early life histories of slipper lobsters. *In*: The Biology and Fisheries of the Slipper Lobster, pp. 69–90.

Shen H, Braband A, Scholtz G. 2013. Mitogenomic analysis of decapod crustacean phylogeny corroborates traditional views on their relationships. Mol Phylogenet Evol **66(3):**776–789. doi:10.1016/j.ympev.2012.11.002.

Singh SP, Groeneveld JC, Al-Marzouqi A, Willows-Munro S. 2017. A molecular phylogeny of the spiny lobster *Panulirus homarus* highlights a separately evolving lineage from the Southwest Indian Ocean. PeerJ **5:**e3356. doi:10.7717/peerj.3356.

Spanier E, Lavalli K. 2007. Slipper lobster fisheries — present status and future perspectives. *In*: The Biology and Fisheries of the Slipper Lobsters, pp. 377–391.

Spanier E, Lavalli K. 2013. Commercial scyllarids. *In*: Lobsters: Biology, Management, Aquaculture and Fisheries, pp. 414–466. doi:10.1002/9781118517444.ch13.

Takahashi M, Saisho T. 1978. The complete larval development of the scyllarid lobster, *Ibacus ciliatus* (von Siebold) and *Ibacus novemdentatus* Gibbes in the laboratory. Mem Fac Fish Kagoshima Univ **27(1):**305–353.

Tam YK, Kornfield I. 1998. Phylogenetic relationships of clawed lobster genera (Decapoda: Nephropidae) based on mitochondrial 16S rRNA gene sequences. J Crustac Biol **18(1):**138–146. doi:10.1163/193724098X00142.

Ueda K, Yanagimoto T, Chow S, Kuroki M, Yamakawa T. 2021. Molecular identification of mid to final stage slipper lobster phyllosoma larvae of the genus *Chelarctus* (Crustacea: Decapoda: Scyllaridae) collected in the Pacific with descriptions of their larval morphology. Zool Stud **60:**75. doi:10.6620/ZS.2021.60-75.

Vogler AP, Monaghan MT. 2007. Recent advances in DNA taxonomy. J Zool Syst Evol Res **45(1):**1–10. doi:10.1111/j.1439-0469.2006.00384.x.

Wakabayashi K, Phillips BF. 2016. Morphological descriptions of laboratory reared larvae and post-larvae of the Australian shovel-nosed lobster *Thenus australiensis* Burton & Davie, 2007 (Decapoda, Scyllaridae). Crustaceana **89(1):**97–117. doi:10.1163/15685403-00003511.

Wakabayashi K, Tanaka Y, Abe H. 2017a. Field Guide to Marine Plankton. Tokyo: Bun-Ichi.

Wakabayashi K, Yang CH, Chan TY, Phillips BF. 2020. The final phyllosoma, nisto, and first juvenile stages of the slipper lobster *Petrarctus brevicornis* (Holthuis, 1946) (Decapoda: Achelata: Scyllaridae). J Crustac Biol **40(3):**237–246. doi:10.1093/jcbiol/ruaa013.

Wakabayashi K, Yang CH, Shy JY, He CH, Chan TY. 2017b. Correct identification and redescription of the larval stages and early juveniles of the slipper lobster *Eduarctus martensii* (Pfeffer, 1881) (Decapoda: Scyllaridae). J Crustac Biol **37(2):**204–219. doi:10.1093/jcbiol/rux009.

Webber WR, Booth JD. 2007. Taxonomy and Evolution. *In*: The Biology and Fisheries of the Slipper Lobster, pp. 25–52.

Wong KJH, Tsao YF, Tsai PC, Hsieh WP, Li HR, Machida RJ, Chan BKK. 2021. To the light side: molecular diversity and morphology of stomatopod larvae and juveniles (Crustacea: Malacostraca: Stomatopoda) from crustose coralline algal reef in Taiwan. Mar Biodivers **51:**20(1–31). doi:10.1007/s12526-020-01150-z.

Woodings LN, Murphy NP, Jeffs A, Suthers IM, Liggins GW, Strugnell JM. 2019. Distribution of Palinuridae and Scyllaridae phyllosoma larvae within the East Australian Current: a climate change hot spot. Mar Freshw Res **70(7):**1020–1033. doi:10.1071/MF18331.

WoRMS 2021. Scyllaridae Latreille, 1825. Available at: http://www.marinespecies.org/aphia.php?p=taxdetails&id=106795. Accessed 31 July. 2021.

Yang CH, Bracken-Grissom H, Kim D, Crandall KA, Chan TY. 2012. Phylogenetic relationships, character evolution, and taxonomic implications within the slipper lobsters (Crustacea: Decapoda: Scyllaridae). Mol Phylogenet Evol **62(1):**237–250. doi:10.1016/j.ympev.2011.09.019.

Yoneyama S, Takeda M. 1998. Phyllosoma and nisto stage larvae of slipper lobster, *Parribacus*, from the Izu-Kazan Islands, Southern Japan. Bull Nat Sci Mus Ser A **24(3):**161–175.

Yoshimoto A, Moritaki T, Saito N, Wakabayashi K. 2020. A new species of *Dendrogaster* Knipowitsch, 1890 (Thecostraca: Ascothoracida: Dendrogasteridae) parasitic in the sea star *Certonardoa semiregularis* (Müller & Troschel, 1842) (Echinodermata: Asteroidea) from Japan. J Crustac Biol **40(6):**795–807. doi:10.1093/jcbiol/ruaa040.

Supplementary materials

Table S1. K2P genetic distances of the partial sequences of *COI* (lower) and *16S* (upper). Standard errors were $P < 0.028$. Blue columns show the distances within a species. See figure 2 caption for the meaning of hash (#), delta (Δ), and asterisk (*) symbols. (download)